# $CaTiAlO_4$ Spinal Ceramic Nano Ovals: Synthesis, Physicochemical Characterization and Antimicrobial Activity with Water Remediation Application

**Patil M.V.[1*], Bamane S.R.[2] and Khetre S.M.[3]**
1. Department of Chemistry, Miraj Mahavidyalaya, Miraj-416410, INDIA
2. Sushila Shankarrao Gadave Mahavidyalaya, Khandala, Satara-416416, INDIA
3. Department of Chemistry, Dahiwadi College, Dahiwadi, Satara-416416, INDIA
[*]pramanikpatil@rediffmail.com

## *Abstract*

*Oval shaped $CaTiAlO_4$ nanoparticles were synthesized by wet chemical co precipitation and muffle ignition method. The oval shapes of nanomaterial were confirmed using SEM imaging and spinal packing in crystals were determined on the basis of XRD spectrum. The surface functionalities over nanomaterial was confirmed using FTIR spectrum elucidating hydroxyl and oxide groups over surface for future water wetability.*

*Furthermore the porous nature and electronic states in nanomaterial were elaborated on the basis of UV-Vis. And PL spectral transitions along with matching SEM and XRD data. The very high porosity of this ceramic nanomaterial was confirmed by BET measurements and future water remediation applications were demonstrated using antimicrobial testing on Staphylococcus Aureus and membrane water purification activity. Overall this novel ceramic porous nano material has proved useful application in water purification membranes.*

**Keywords:** Oval ceramic, Nano material, Highly Porous, Water remediation, Absorbance.

## Introduction

With the idea in the field of ceramic water nanotechnology, here in this research work we had developed a new class of trio oval metal oxide ceramic nanocomposite material for microbial remediation of surface water resources. Calcium and titanium based materials are used nowadays for antimicrobial applications in various fields.[19,20,26,33] Along with sodium it can form stable mix metal oxide to result in trio metal ceramic type material with good expected porosity. Porosity is mainly important for water remediation and antimicrobial effects of bacterial cell adhesion. So here in this research work we had synthesized this mixed metal oxide ceramic nanocomposite for such porosity required for antimicrobial effects and future water remediation applications.[1,3,6]

Nano technology has emergent research fields which are growing towards development of new class of ceramic metal oxide materials used for water remediation. Ceramic metal oxide nanoparticles and nano composites are having suitable applications for antimicrobial and cleansing of water pollutants and agents. Limited number of reports have been attempted and published by researchers in this field.[17,19,20] So there is need of development of new class of cheaper and suitable nanocomposite mix metal oxide ceramic material to kill microbial contents of water resources to generate good quality of potable water[6,11,15,30].

Hydrogen peroxide is the major theme for this application of ceramic nanocomposites as these materials generate peroxide entities with porous surface in water[14]. Oval ceramic material can be used not only for antimicrobial application but also for water remediation.

## Material and Methods

All the chemicals used for synthesis for nanocomposites and their *in vitro* biological screening such as aluminium nitrate, titanium chloride, calcium nitrate, conc. HCl and ethanol were of A. R. grade. These chemicals were purchased from S. D. Fine Chem. Ltd. and Merck and were used without further purification. The cell culture medium such as agar growth broth and bacterial culture, fetal bovine serum, trypsin buffer were obtained from Hi Media Ltd. The double distilled water was obtained from Millipore system and used throughout the synthesis and *in vitro* biological screening tests.

### General procedure

**Synthesis of oval ceramic nanoparticles:** All the metal salts are mixed in 0.01M proportion in 25 ml. double distilled water and traces of HCL are added to the flask. The flask contents are vortexed on magnetic stirrer at 600 rpm. for 6 hours. Visible color change was observed after formation of precipitate. The precipitate was washed with double distilled water and dried in oven at $92^{O}C$. The dried trio metal oxide nano composite ceramic powder was then crushed and bonded with gluteraldehyde binder to form pallet. This powder and pallet were characterized and used for antimicrobial studies in water remediation.

**Co-precipitation method:** For this experimental detection, co-precipitation method is used. The advantage of the co precipitation method involve simplicity and rapid preparation, composition and particle size control, energy efficiency, low temperature and homogeneity of particles. There are three main mechanism of co-precipitation: inclusion, occlusion and adsorption.

**Structural and morphological characterization of oval nanomaterial:** As mentioned in table 1, the structure, morphology, particle diameter range and types of bonding of functionalities in the ceramic nanocomposite was

determined based on physicochemical characterization using UV-Vis., PL, FTIR, XRD spectrometry techniques and SEM microscopic analysis.[2,8-10,36] The Spectronics double beam UV-Vis. spectrometer with water as blank was used to determine absorption spectrum of material.

To confirm functionalities present in material and comparing with pallet form, Perkin Elmer series FTIR spectrometer was used with KBr pellet technique. The PL emission spectrum of nanocomposite was determined using Jusco type spectra fluorometer with excitation identity of material with same 25 ppm concentrations. The X-ray diffraction pattern of material was determined using X-ray spectrometer by powder diffraction technique to elaborate the packing f ions, hybridization and crystal system of nanocomposite entities. The composition of material, formation and phase of ceramic nanocomposite is proved here by this spectrometric analysis.

**Antimicrobial screening on gram positive bacteria by agar well disc diffusion method:** The cell-particle interactions of materials demonstrating their reactivity and biocompatibility can be elaborated using simple *in vitro* antibacterial screening in buffer solutions to maintain physiological mimicking pH at material cell interactions. As cell pH affect on the biocompatibility of molecules. Here in this work 20 ppm. concentrations of material were dosed on bacterial cell cultures grown in agar broth on discs, inside the wells bored on plates. The gram positive *Staphylococcus Aureus* bacteria was grown on culture plates and inhibited by dosing of material solutions in buffer dispersions with physiological pH = 7.4 by use of phosphate buffer [26]. The culture plates were incubated and zones of inhibition were measured and biocompatibility/ antimicrobial property of nanocomposite was elaborated.

## Results and Discussion

**Morphological and structural characterization of ceramic nanomaterial**

**UV-vis Absorption and pl emission spectrum:** The UV-vis region of energy for electromagnetic spectrum at wavelength range from 200nm to 400nm. Absorbance or emission peak shown in fig. 1 of UV-Vis spectrum is due to Schiff base transition[21,24,25] results in metal CORM complex charge transfer transition. The UV-Vis absorption at 209.5 nm is due to n to pi absorption maxima in which charge transfer takes place $A_1g$ to $T_1g$ and $A_2g$ to $T_2g$ from d5 state of Ti and Al for splitting from bonding of carbimide and CO species. PL g at 222 nm is due to n to Pi relaxation in which charge transfer takes place Pi to Pi relaxation- no quenching due to Ti, Al oxide.

The composition of material, formation and phase of ceramic nanocomposite was proved here by spectrometric analysis.

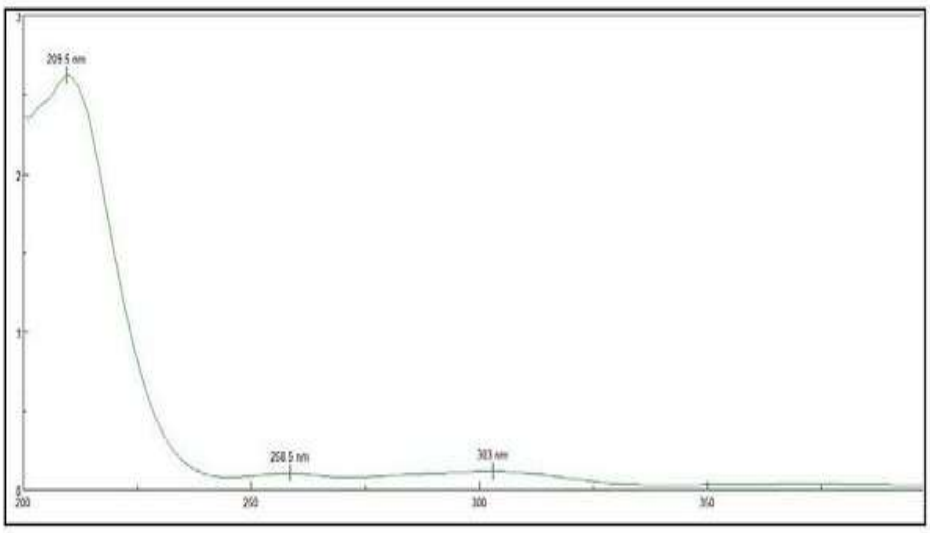


**Figure 1: UV-Visible absorption spectrum of $CaTiAlO_4$ ceramic nanomaterial**

**Table 1**
**MLCT transitions of non bonded/ Pi electrons of ligands and d electrons of metals**

| Absorption or emission peak shown in UV-Vis. Or PL spectrum | Schiff base transition | Metal CORM complex charge transfer transition |
|---|---|---|
| UV-Vis. Absorption at 209.5nm. | n to Pi absorption maxima | $A_{1g}$ to $T_{2g}$ and $A_{1g}$ to $A_{2g}$ from $d^5$ state of Ti ans Al for splitting from bonding of carbimide and CO species |
| PL g at 222 nm. | n to Pi relaxation- no quenching | Pi to Pi relaxation – no quenching due to Ti, Al oxide |

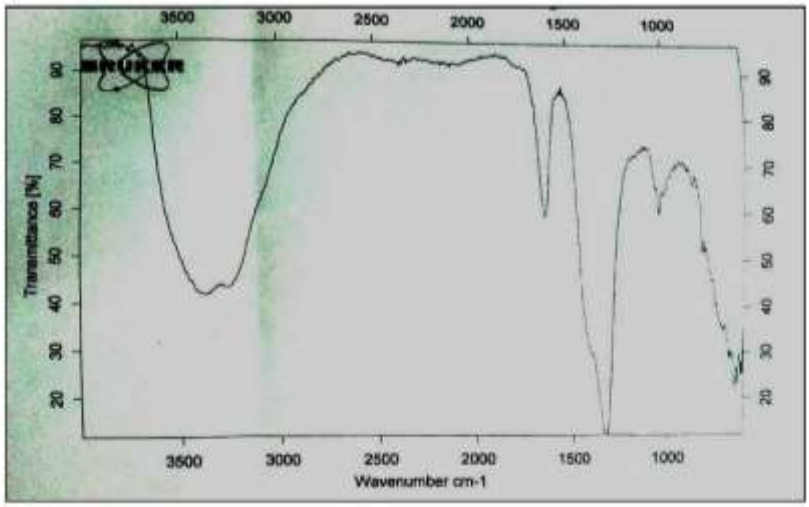


**Figure 2: PL emmission spectrum of $CaTiAlO_4$ disc Nanomaterial**

**Table 2**
**Matching of FTIR signals elaborating the functionalities of Schiff base and CORM complex**

| Signal in FTIR spectrum | Functionality | Ceramic group functionality |
|---|---|---|
| 483 $cm^{-1}$ | Ca-Al linkage | Metal-oxide bonds |
| 828 $cm^{-1}$ | Al-O linkage | Presence of linked oxide metal species |
| 1050 $cm^{-1}$ | Ti-Al group | Metal (I) and Metal (III) interaction |
| 1385 and 1663 $cm^{-1}$ | Presence of hydroxide | Surface groups of oxide nanomaterial |
| 1764 and 3222 $cm^{-1}$ | Presence of –OH and Oxides | Presence of surface moisture for porosity |

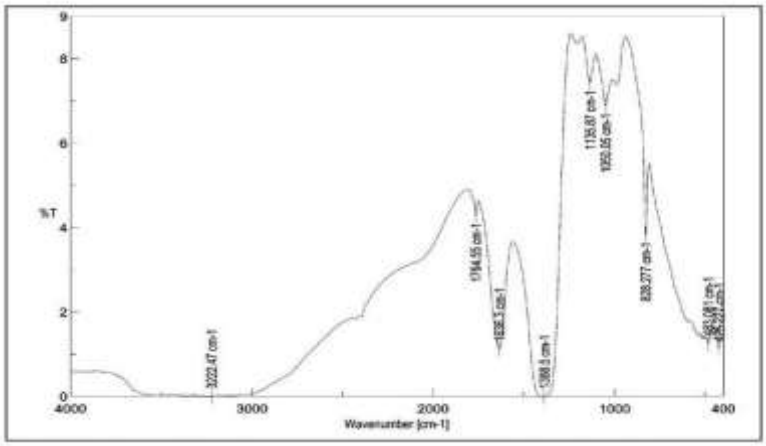


**Figure 3: FTIR spectrum of $CaTiAlO_4$ ceramic nanomaterial for surface functionalities**

**FTIR spectrum of ceramic nanomaterial for surface functionalities:** FTIR spectrum of ceramic nanomaterial CaTiAlO4 is shown in fig. 3 and table 2. With the help of it we can find surface groups.[12,24,32]

**XRD (X- RAY diffraction) pattern of trio metal nanomaterial:** X-ray diffraction study of $CaTiAlO_4$ ceramic nano material sample was examined by XRD analysis [10,13,35].Fig. 4 shows x-ray diffraction pattern of $CaTiAlO_4$ ceramic nano material sample analyzed at different temperatures $^0$C. The XRD analysis of this sample contain similar pattern with each other except change in peak height and peak with increase in temperatures. This pattern correspond to peak of (101), (221), (242), (211), (412). As per XRD data in fig. 4, it has been proved that the ceramic nano composite material has octahedral packing of ions and cubic phase purity elaborated 65nm size from main peak by using Schere's equation:

$$d= a/\sqrt{h^2+k^2+1^2} \quad (1)$$

As per XRD data in figure 3 and table 3, it had been proved that the ceramic nanocomposite has octahedral packing of ions and cubic phase purity elaborating the 65 nm sizes from main peak using Scherer's equation.

**SEM image for disc morphology:** The SEM image of nanocomposite ceramic was shown in figure 5. It throws light on Oval shapes of material with some aggregation of particles. This trio metal oxide ceramic composite possess not only porosity but also exhibits Oval shapes for better water loving nature and cell particle interactions.

**BET isotherm elaborating porosity of disc nanomaterial:** As per fig. 6, it is oberved that the ceramic nanocomposite show multi layer BET isotherm for nitrogen adsorpion hence it has good surface posrosity. The BET plot hence proved presence of porosity on surface of this nanocomposite ceramic material.[9]

**Table 3**
**Crystal parameters of Ceramic nanocomposite with octahedral packing matched with known ceramic JCPDS card.**

| Crystallite planes (Miller Indices) (h,k,l) Main peaks of ceramic nano trio metal oxide | d Calculated $A^0$ $d = a/\sqrt{(h^2+k^2+l^2)}$ or $2dSin\theta = n\lambda$ | d Standard $A^0$ JCPDS card no.- 86-6788 for $CaTiAlO_4$ matched | Lattice Constant a and b $A^0$ from main XRD peaks [242] at theta = 37.5 of disc ceramic nanomaterial |
|---|---|---|---|
| 101 | 4.324 | 4.345 | a standard = 5.249 |
| 221 | 5.453 | 5.456 | b standard = 7.266 |
| **242** | **7.234** | **7.230** | |
| 211 | 4.986 | 4.988 | a calculated = 5.251 and |
| 412 | 6.789 | 6.785 | b calculated = 7.272 |

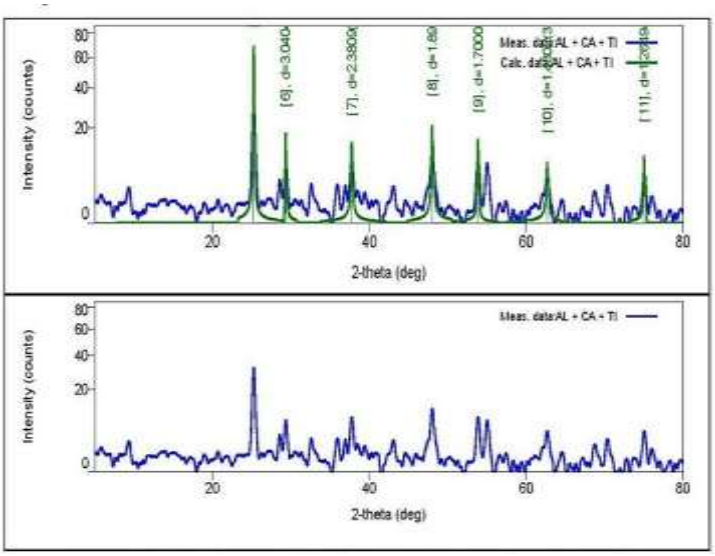


**Figure 4: XRD pattern of the disc $CaTiAlO_4$ ceramic nanomaterial**

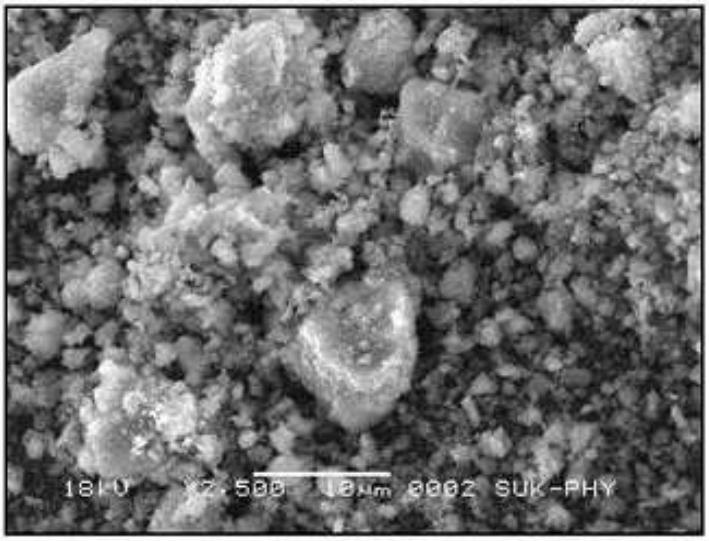


**Figure 5: SEM image of $CaTiAlO_4$ nanomaterial with oval morphology**

**Antimicrobial properties for water remediation from nanomaterial:** As per figure 7 and table 4, for antimicrobial activity of 20 ppm material on *Staphylococcus aureus*, it had been demonstrated that good zone of inhibition was having better antimicrobial activity.[26,36]

**Mechanism for antimicrobial activity and water remediation activity:** As per physicochemical and antimicrobial screening of material and elaboration in scheme 1, the disc nanomaterial trio metal oxide ceramic nanocomposite exhibit antimicrobial and water remediation potential at surface by material cell interactions. Here as material had surface porosity after reaction with cell membrane material and water, the surface of material shows adhesion to liquid and biomaterials which result in dissociation of nanocomposite to oxides on surface, resulting in production of peroxide on surface. This peroxide produced at surface of nanomaterial further can produce oxide and super oxide radicals to give antimicrobial effects for water remediation activity.[26,36]

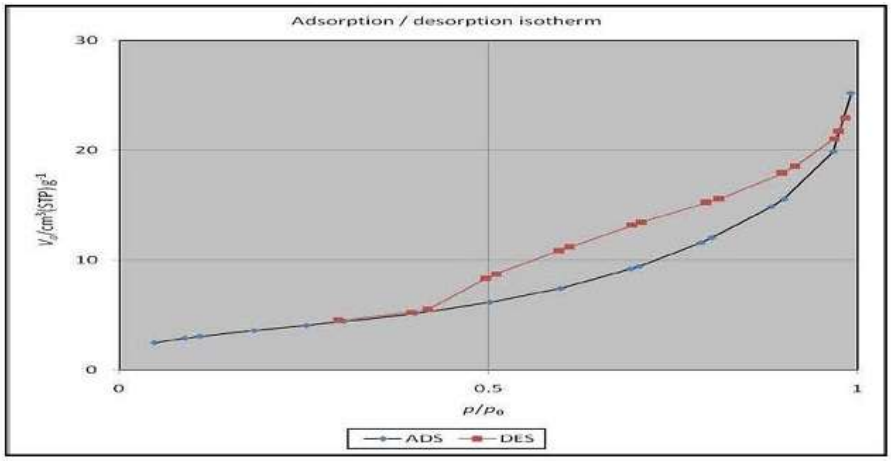


**Figure 6: BET adsorption isotherm of $CaTiAlO_4$ nanomaterial elaborating surface porosity**

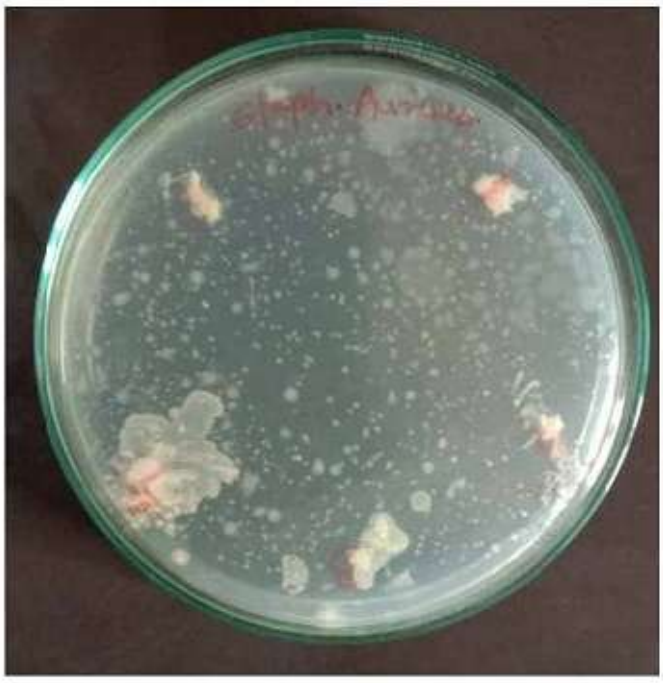

**Figure 7: Anti microbial effects of ceramic nanomaterial on *Staphylococcus Aureus* for zone of inhibition at 20 ppm.**

**Table 4**
**Anti microbial activities of Schiff base and complex compared for gram positive and gram negative bacteria.**

| Type/ name of bacterial culture in Agar broth [as per figures] | Zones of inhibition for gram positive bacteria as zone diameter in mm. for Concentrations of drug/ dose of ceramic nanomaterial | |
|---|---|---|
| | At 10 ppm. | At 25 ppm Fig. 7 |
| *Staphylococcus Aureus (gram +ve)* | 15 mm. | 27 mm. |

**Water remediation activity of $CaTiAlO_4$**

**Explanation**: The photo catalytic degradation of methylene blue dye in CaTiAlO4 mixed oxide ceramic suspension under UV light elimination was investigated in order to evaluate its photo catalytic activity[18,32]. A reaction system was setup at 20ppm concentration and 150 mg/100ml photo catalysts amount. Sample is observed in total 180 min in photo catalytic multi lamp reactor with UV light (365 nm Hg Vapor lamp) with maximum emission at about 660 nm at room temperature at constant starring to maintain homogeneous suspension. The suspension was irradiated for 30 min to 3 hrs. period. The suspension was withdrawn and centrifuge at each time of interval to remove $CaTiAlO_4$ particles.

The absorption of methylene blue dye solution was measured using UV-visible Spectrophotometer at its characteristics wavelength. The percentage degradation of methylene blue dye at irradiated time interval was calculated by using following equation:

$$\text{Degradation Percentage} = \left(1 - \frac{At}{Ao}\right) \text{ x } 100$$

where A is absorbance after time‘t’ and Ao is absorbance of dye solution before degradation.

It has been observed that at 180 min. Methylene blue dye shows 68% degradation rate. The absorption band gap of $CaTiAlO_4$ is 3.63 eV indicating that ceramic nano catalyst CaTiAlO4 is suitable and best catalyst for degradation of methylene blue dye result in removal of polluted elements from water resources.

**Table 5**
**Degradation Parameters**

| | | |
|---|---|---|
| 1. | Dye | Methylene Blue |
| 2. | Concentration | 20 ppm |
| 3. | Photo catalyst’s amount | 150mg/100mL |
| 4. | Degradation Time | 180 min |
| 5. | Degradation Efficiency | 68% |
| 6. | pH | 7 |
| 6. | Source of light | 365 nm Hg Vapor lamp |

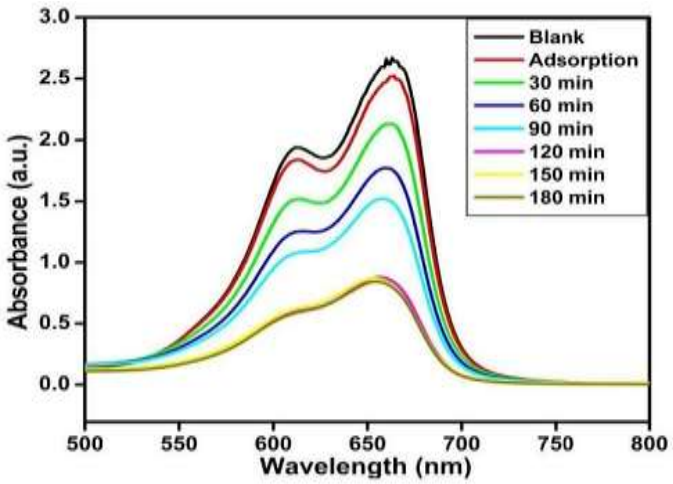


**Fig. 8: % Degradation of Methylene Blue Dye with catalyst $CaTiAlO_4$**

**Table 6**
**% degradation during course of time**

| Time | % Degradation of MB |
|---|---|
| Blank | 00 |
| Adsorption | 5 |
| 30 min | 19 |
| 60 min | 33 |
| 90 min | 42 |
| 120 min | 66 |
| 150 min | 67 |
| 180 min | 68 |

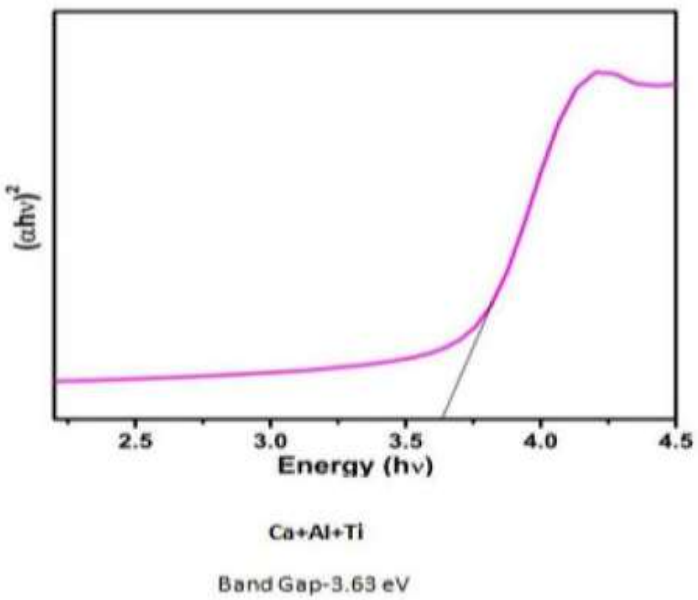


**Fig. 9: Absorbance Band gap of $CaTiAlO_4$**

## Conclusion

A new disc shaped trio metal oxide based ceramic nanomaterial was prepared using simple wet chemical and drying route. This nanomaterial with 55 nm mean size had exhibited surface porosity on the basis of BET isotherm $N_2$ adsorption. The absorption and emission spectra of nanomaterial had proved presence of oxide free electrons on surface. The nanomaterial possess surface oxide and hydroxide species for water loving nature of material on the basis of FTIR analysis.

On the basis of antimicrobial testing of the material, it has been determined that this oval ceramic trio metal oxide nanomaterial finds applications in water purification and environmental fields.

## Acknowledgement

The authors are thankful to Analytical Instrumentation Laboratory, DST-FIST, Jaysingpur College, Jaysingpur, India for providing some spectroscopic characterizations of samples and Department of Microbiology, Miraj Mahavidyalaya, Miraj for providing cell cultures and *in vitro* testing facilities. We are also thankful to Principal, Miraj Mahavidyalaya, Miraj and Principal, Dahiwadi College, Dahiwadi for encouragement.

## References

1. Amorelli A., Evans J.C. and Rowlands C.C., *J. Chem. Soc., Faraday Trans.*, **84**, 1723 **(1988)**

2. Baran W. and Makowasky A., *Dyes and Pigments*, **76**, 226-230 **(2008)**

3. Binet C. and Daturi M., *Catal. Today*, **70**, 155 **(2001)**

4. Barwell C.N. and McCash E. Mo, Fundamentals of molecular spectroscopy, Fourth Edition, Tata, Mc-Graw-Hill. Publishing Company Limited **(2017)**

5. Bragg W.H., The structure of the spinel group of crystals, *Phil. Mag.*, **30(176)**, 305 **(1915)**

6. Buxton G.V., Greenstock C.L., Helman W.P. and Ross A.B., *J. Phys. Chem. Ref. Data*, **17**, 513 **(1988)**

7. Crewe Albert V., Isaacson M. and Johnson D., *Rev. Sci. Instrum*., **40(2)**, 241-246 **(1969)**

8. Connes J. and Connes P., *Instruments and Results*, **56(7)**, 896-910 **(1966)**

9. Condon J., Surface Area and Porosity Determination by Physisorption; Measurement, Classical Theory and Wuantum Theory, 2nd ed., Amsterdam, Chapters 3, 4-5 **(2020)**

10. Cullity B.D., elements of X-ray diffraction, Addison-Wesley, California, USA, 2nd ed., 102 **(1978)**

11. Egerton R.F., Physical Principles of Election Microscopy: An Introduction to TEM, SEM and AEM, Springer, 125-153 **(2005)**

12. Fujishima A. and Zhang X., *CR Chimie*, **9**, 750-760 **(2006)**

13. Fultz Bo and Howe J., Transmission Election Microscopy and Diffractometry of materials, Springer **(2007)**

14. Giamello E., Volante M., Fubini B., Geobaldo F. and Morterra C., *Mater. Chem. Phys.*, **29**, 379 **(1991)**

15. Giamello E., Calosso L., Fubini B. and Geobaldo F., *J. Phys. Chem*., **97**, 5735 **(1993)**

16. Ghormely J.A. and Stewart A.C., *J. Am. Chem. Soc*., **78**, 2934 **(1956)**

17. Gupta A.K., Pal A. and Sahoo C., *Dyes and Pigments*, **69**, 224-232 **(2006)**

18. Haines R.I., McCracken D.R. and Rasewych J.B., In Water Chemistry of Nuclear Reactor Systems 5, British Nuclear Energy Society, London, 309 **(1989)**

19. Hochanadel C.J., *J. Phys. Chem*., **56**, 587 **(1952)**

20. Hawkes P., ed., The beginnings of Electron Microscopy, Academic Press **(1985)**

21. The Infracord double-beam spectrophotometer, *Clinical Science*, **16(2) (1957)**

22. Kingery W.D., *Archaeometry*, **16**, 109-112 **(1976)**

23. Lee R.E., Scanning electron microscopy and x-ray microanalysis, PTR Prentice Hall, Englewood Cliffs, New Jersey **(1993)**

24. Lewes G., Scanning electron microscopy and X-ray microanalysis, John Willey and Sons, UK **(1987)**

25. Matai I., Sachdev A., Dubey P., Kumar S.U., Bhushan B. and Gopinath P., *Colloids Surf B Biointerfaces*, **115**, 359-367 **(2014)**

26. McCracken D.R., Tsang K.T. and Laughton P.J., Aspects of the Physics and Chemistry of Water Radiolysis by Fast Neutrons and Fast Electrons in Nuclear Reactors, AECL 11895, Atomic Energy of Canada Limited, Chalk River, CA **(1998)**

27. McMullan D., *Scanning*, **17(3)**, 175-185 **(2006)**

28. Misra P. and Dubinski M., eds., Ultraviolet Spectroscopy and UV Lasers, New York, Marcel Dekker **(2002)**

29. Novak E., Hancz A. and Erdohelyi A., *Radiat. Phys. Chem*., **66**, 27 **(2003)**

30. Goldstein J., Scanning Electron microscopy and - X-ray Microanalysis, Plenum Publishers, 68 **(2003)**

31. Pillai V., Lonkar S. and Alhassan S., *ACS Omega*, **5(14)**, 7969-7978 **(2020)**

32. Ramachandran V.S., Applications of differential thermal analysis in Cement Chemistry, Chap. V, Chemical Publishing Co., Inc., New York, 92 **(1969)**

33. Reimer L., Scanning Electron Microscopy: Physics of Image formation and Microanalysis, Springer, 527 **(1998)**

34. Schuler R.H. and Allen A.O., *J. Phys. Chem.*, ***24***, 56 **(1956)**

35. Sondi I. and Salopek-Sondi B., *J Colloid Interf Sci*., **275(1)**, 177-182 **(2004)**

36. Spence J.H., High-resolution electron microscopy, Oxford press **(1980)**

37. Suryanarayana C. and Norton M., X-ray Diffraction: A Practical Approach **(2013)**

38. Westgren A. and Phragmers G., X-ray Analysis of the Cu-Zn, Ag-Zn and Au-Zn Alloys, *Phil. Mag*., **50**, 311 **(1925)**

39. Williams D. and Carter C.B., Transmission Electron Microscopy 1- Basics, Plenum Press **(1996)**

40. Zhu J., Gao J. and Wang Y., Synthesis of highly active H2O2 sensitized sulfated titania nanoparticles with a response to visible light, *J Photochem Photobiol A: Chem*., **202**, 128-135 **(2009)**

41. Zworykin V.A., Hillier J. and Snyder R.L., A Scanning electron microscope, *ASTM Bull*., **117**, 15-23 **(1942)**.

(Received 05th February 2021, accepted 10th March 2021)